Available online at www.sciencedirect.com
SCIENCE DIRECT
Polymer 46 (2005) 11311–11321
polymer
www.elsevier.com/locate/polymer

# Surface energy inducing asymmetric phase distribution in films of a bynary polymeric blend

Monica Bertoldo [a,*], Maria Beatrice Coltelli [a], Lidia Miraglia [b], Piero Narducci [c], Simona Bronco [a]

[a] Polylab-INFM, Department of Chemistry and Industrial Chemistry, University of Pisa, via Risorgimento 35, 56126 Pisa, Italy
[b] Department of Chemistry and Industrial Chemistry, University of Pisa, via Risorgimento 35, 56126 Pisa, Italy
[c] Engineering Chemistry Department, University of Pisa, via Diotisalvi, 2, 56126 Pisa, Italy

Received 24 March 2005; accepted 7 October 2005
Available online 27 October 2005

**Abstract**

The phase morphology of blends of low density polyethylene (PE) with low molecular weight copolyamide (CPA) was investigated in films having 50–100 μm thickness. Films were prepared by compression moulding between two surfaces with different polarity, namely teflon and aluminium sheets, in a parallel plate heating press. The film surface characterization and surface energy deduction were performed by FT-IR/ATR spectroscopy and contact angle measurements, respectively. Moreover, the morphology and phase distribution were investigated by scanning electron microscopy both on the surfaces and on the cryogenic section of the films.

The copolyamide resulted to be the dispersed phase in all compositions (90/10, 95/5, 97.5/2.5 and 99/1 PE/CPA) and the shape, dimension and distribution of the domains depending on temperature, pressure, time and nature of the surfaces used during the compression stage.

The experimental evidences were discussed with respect to the different surface energies of the type of moulding material during the film preparation and related compatibility of the components.


*Keywords:* Polyethylene blends; Surface energy; Polyethylene/copolyamide films

## 1. Introduction

The bulk and surface phase morphology in multicomponent materials, such as blends, alloys and laminates usually depends on interface interactions among the phases and affects the final performances such as stiffness, fracture resistance, shockproof properties and stability to delamination [1–3]. On the other side, the morphologic properties such as the dispersion and dispersed phase diameter in blends are affected by the processing conditions, e.g. rotor speed or mixing time, adopted to produce the blend [4]. The kind of processing can affect the morphology in correspondence of object surface as observed in HDPE/PA6 blends where the dispersed phase was highly oriented in the subskin and assumed a spherical shape in the core as an effect of the different shear flow [5]. Moreover, the minor phase (HDPE) appeared absent in the skin in good agreement with the surface composition of PP/PET blends compression moulded between polyimide surfaces [6]. In the latter case, the preferential PP displacement into the bulk in a PET matrix blend was attributed to a poor affinity of the dispersed phase for the moulding surface.

A morphology evolution of the labeled EPR (HY-EPR) by spinodal decomposition similar to those usually observed in very thin films (thickness $<0.1$ μm) was reported for PE/PP/EPR ternary blend films with a thickness of 100 μm annealed at 175 °C between surfaces at different polarity [7,8]. A lamellar morphology was found in films annealed for long time between surfaces made by stainless steel or PP with the draining of the HY-EPR/PE core shell phase from the PP interface. The phase separation evolved by hydrodynamic channels and was driven by the wetting of the stainless steel moulding surface. A similar behavior was reported for a PP/EPR blend [9] and for films made by a polybuthene/polyisoprene blend [10]. In particular a percolating phase morphology parallel to the surface was observed in films annealed on glass plates and having a thickness of 0.5 μm [10].

Several papers deal with the influence of surface on establishing the miscibility between blend components and the derived morphology in thin films, included the dewetting phenomena ruled by the interface interactions [11–25]. The thin films features can not be predicted only on the basis of the

* Corresponding author. Tel.: +39 502219413; fax: +39 502219320.
*E-mail address:* monicab@dcci.unipi.it (M. Bertoldo).

0032-3861/$ - see front matter © 2005 Elsevier Ltd. All rights reserved.
doi:10.1016/j.polymer.2005.10.040

bulk properties [11,12] as the surface is not negligible and modifies the thermodynamic equilibrium of the whole system [18,26,27]. This chain confinement is felt at distances bigger than a single chain length and gives rise to phase separation and surface segregation that are not usually observed in the bulk [13]. In other cases, the interaction of a blend component with a surface makes miscible polymers otherwise immiscible [11]. The component of a binary blend having the lowest surface energy usually segregates preferentially at the polymer–air interface. This effect increases as the difference in the surface energy between the components becomes larger in spite of the decreasing component compatibility. This is not always true for films obtained by solvent casting or spin coating because the surface enriches in the most compatible solvent component [28,29]. The segregation is strongly influenced by the molecular weight of the polymers [1], because the surface energy increases as this parameter increases, and by the presence of crystallisable polymer chains because of the competition among the amorphous phase segregation, the crystallisation and the phase separation [30,31].

In this paper, with the aim at achieving polyethylene based materials able to self stick onto polar surfaces just by heating, a new experimental approach taking advantage of the phenomena of surface segregation was exploited. The possibility of influencing the distribution of the minor phase in moderate thick films (50–100 μm) made of polyethylene/copolyamide binary blends prepared by compression moulding was investigated. Materials of different polarity, namely teflon and aluminium, were used as moulding surfaces. The surface characterization of all prepared films and the surface energy evaluation of all used materials were carried out by FT-IR/ATR spectroscopy and contact angle measurements. Moreover, the effect of blend composition, processing temperature, time and pressure on morphology, distribution and orientation of the dispersed phase were investigated by scanning electron microscopy both on the surfaces and on the cryogenic sections of the films. The results are discussed on the basis of the different interfacial energy of the material pairs.

## 2. Experimental

### 2.1. Material

Low density polyethylene (PE) pellets (density 0.925 g/cm$^3$, vicat softening point 98 °C, $\bar{M}_w$ 186,000, $\bar{M}_n$ 41,000) was an Exxon Mobil polyethylene LD 158 JD commercial product. The so called copolyamide (CPA) is a commercial hot-melt adhesive (Degussa, Vestamelt X1017/25) derived from the copolymerization of ε-caprolactame and ω-laurolactame with a minor amount of methyl branched units [$CH_2/CH_3$ from $^1$H NMR = 56]. It is characterized by: melt index 250 g/10 min, melting point 117 °C and (thermal stability at $T < 400$ °C) degradation onset temperature of 415 and 435 °C in air and nitrogen flow, respectively.


Fig. 1. Schematic drawing of the assembly used to obtain the compression moulded films. In the picture the case is reported where two different rigid sheets (teflon and aluminium) are used as moulding materials.

### 2.2. Films preparation

99/1, 97.5/2.5, 95/5 and 90/10 PE/CPA blends were prepared in a Brabender Plastograph® with a 50 ml mixing chamber at 170 °C by setting 50 rpm as rotor speed and by blending for 10 min. The obtained blends were used to prepare thin films (50–100 μm) by compression moulding of 1.40 g of sample between two rigid sheets in a hydraulic press with plane plates. For each blend three films were moulded: one between two teflon sheets, one between two aluminium sheets and one between a teflon and an aluminium sheet (Fig. 1). All films were quenched at −20 °C in fridge just after the preparation. The films preparation, if not otherwise specified, was carried out at 180 °C, 125 bar for 5 min.

### 2.3. Characterization

The IR spectra were recorded with a Perkin Elmer Spectrum GX equipped with an ATR accessory with SeZn crystal. All ATR spectra were processed with the Spectrum software v. 3.2 and normalised with respect to the adsorption band at 1377 cm$^{-1}$.

The scanning electron microscopy (SEM) analysis of both film surfaces and cryogenic fracture were recorded with a Jeol JSM-5600 LV instrument.

DSC analyses of pure polymer and of their blends were performed with a Mettler Toledo Stare System mod. 822e instrument equipped with a Stare software and liquid nitrogen cooling. Each sample (12–13 mg) were analyzed in the −20/200 °C temperature range with scan rate of 20 °C/min. A cycle simulating the thermal treatment undergone by the blends during the film preparation were performed: the blend was heated to 180 °C and kept at this temperature for 5 min, then was cooled down to −20 °C temperature kept for 10 min and then heated again to 200 °C. The analysis of the second heating step was carried out.

TGA analyses were performed with a Mettler Toledo Stare System mod. 822e instrument equipped with a Stare software under nitrogen or oxygen atmosphere (80 ml/min) on 10–15 mg of each sample. The temperature range of analysis was 25–700 °C and the scan rate of 10 °C/min.

A KSV, CAM 200, optical contact angle meter goniometry was used to measure water and diiodomethane static contact angle by forming 5 μl droplets on the surface of the film at a rate of 0.2 μl/s and two different images were recorded for each drop. An average value was obtained from 5 to 7 measurements for each film sample. The surface energy ($\gamma$) of the pure materials was deduced using the geometric Eq. (1) and assuming the values of 21.80$m$ J/m$^2$ and 51.00$m$ J/m$^2$ for the

Table 1
Surface energy of the used materials

| Materials | $\gamma^p$ (mJ/m$^2$) | $\gamma^d$ (mJ/m$^2$) | $\gamma^a$ (mJ/m$^2$) |
|---|---|---|---|
| PE | 3.5 | 28.6 | 32.1 |
| CPA | 6.6 | 39.2 | 45.8 |
| Teflon | 0.5 | 13.1 | 13.6 |
| Aluminium | 16.0 | 23.5 | 39.5 |

[a] The surface energies were obtained as sum of the polar and dispersive components.

dispersive ($\gamma^d_{LV}$) and polar ($\gamma^p_{LV}$) components of the surface energy of water, respectively [32]. The corresponding values assumed for diiodomethane were 48.50 and 2.30*m* J/m$^2$ [32]. The same experimental conditions previously described for the preparations of blend films were adopted to obtain pure PE and CPA films. Commercial blow moulded poly(ethylene terephthalate) films having a flat surface were used as interfaces in this case.

AFM height images were collected with a self-assembled instrument equipped with a Burleigh Metris 200 controller. Each sample having 9.2×9.2 μm of area was analyzed at 1, 2, 5, and 10 enlargements in non-contact mode with a resonance frequency of 320 kHz and a stabilized/free amplitude of 2/ 4u.a.

The molecular weight of PE was estimated with a Waters GPCV 2000 with a differential refractive index detector coupled with an online capillary viscometer. A four column configuration was adopted: 3 Styrogel HT 6E and 1 Styrogel HT3 columns (diameter = 7.8 mm, length = 300 mm, with a 10 μm dispersed phase made by styrene–divinylbenzene). The analysis temperature was 140 °C, 1,2,4-trichlorobenzene (HPLC-grade) was used as eluent with a flux of 1 ml/min. A calibration curve was established with monodisperse polystyrene standards.

## 3. Results

### 3.1. Surface energies of materials

The surface energy ($\gamma = \gamma^p + \gamma^d$) measurements of the blend components (PE and CPA) and of aluminium and teflon sheets were evaluated through contact angle measurements performed on films with water and diiodomethane. The polar ($\gamma^p$), the dispersive ($\gamma^d$) components of the surface energy values of each material were calculated according to the geometric Eq. (1) (Table 1) [32].

$$\gamma_{LV}(1+\cos\theta) = 2\left(\gamma^d\gamma^d_{LV}\right)^{1/2} + 2\left(\gamma^p\gamma^p_{LV}\right)^{1/2} \quad (1)$$

where $\gamma^p_{LV}$ and $\gamma^d_{LV}$ are the tabulated polar and dispersive components of the surface energies ($\gamma_{LV} = \gamma^p_{LV} + \gamma^d_{LV}$) of the solvents, respectively [32].

CPA has both polar and dispersive components higher than PE and then it has higher surface energy compared to PE.

### 3.2. Surface analysis of pure PE films

A rough surface was observed by SEM analysis in all PE films prepared by compression moulding, independently of the kind of moulding material used and surface of the pressing plate. In Fig. 2 the images of the two sides of a PE film compression moulded between teflon and aluminium are compared. The former seems to exhibit a less flat and uniform surface than the latter.

The AFM analysis of the same surfaces provided the distribution of the roughness depth reported in Fig. 3. The data confirmed the SEM observation and showed a higher average value of the roughness depth on teflon than on aluminium side. In particular the average height value and the peak to peak distance of the teflon side are two times larger than the values obtained for the aluminium side (Table 2).

### 3.3. Blend characterization

The final torque recorded at 10 min value during the blending of PE and CPA decreased with the increasing of the percentage by weight of CPA (Fig. 4) according to its very low viscosity in the mixing conditions.

The DSC and the SEM analysis of all studied blends indicated that PE and CPA are incompatible as expected because of the large difference in surface energy. Despite the

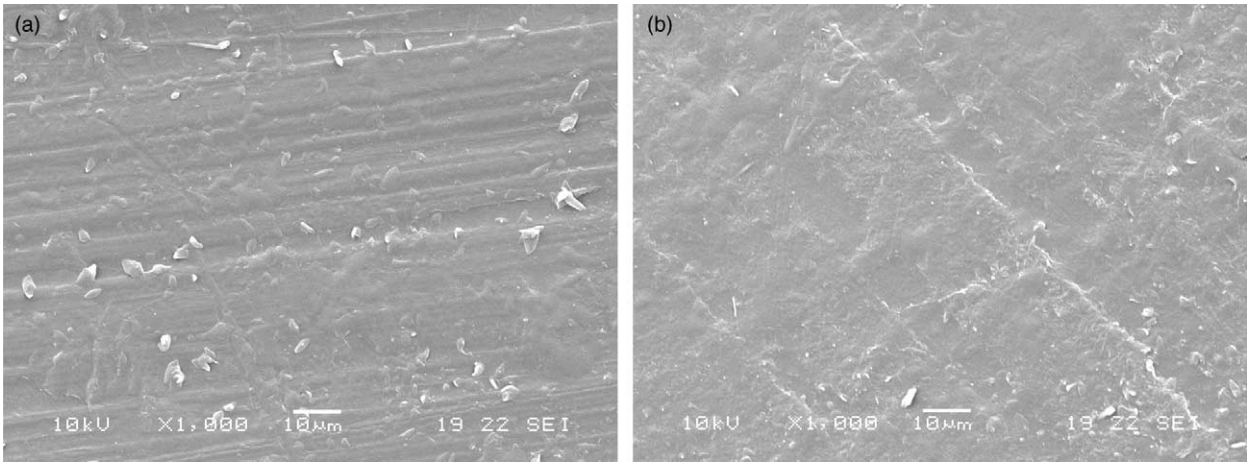


Fig. 2. SEM micrographs of the surfaces of the PE film compression moulded between aluminium and teflon: (a) teflon faced side, (b) aluminium faced side.

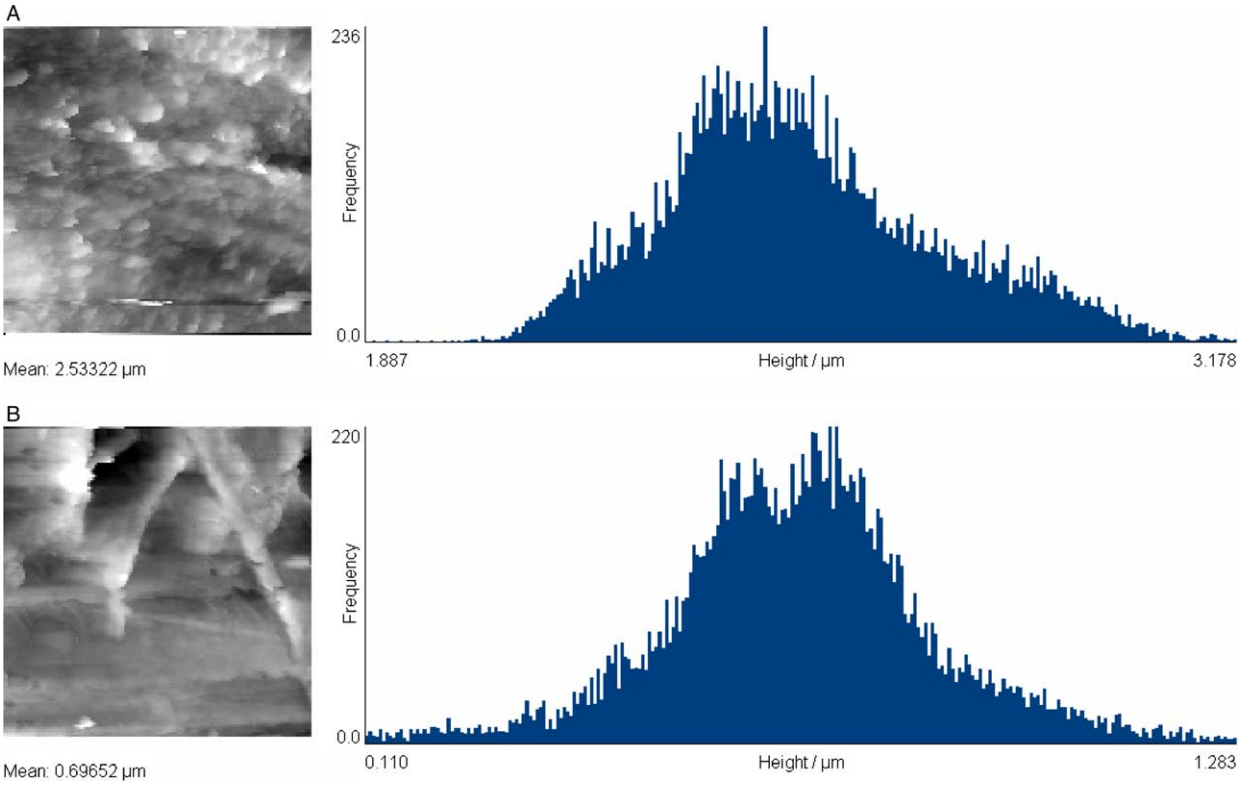


Fig. 3. AFM analysis of the height distribution of the surface roughness of a PE film compression moulded between teflon and aluminium: (a) teflon faced side; (b) aluminium faced side.

superimposition of the melting peaks of pure PE and CPA the DSC curve of the 90/10 blend showed a small peak corresponding to the exothermic transition of pure CPA crystallization (Fig. 5). The presence of this peak indicated the possible existence of separate domains of CPA in the blend. The SEM analysis of the cryogenic fracture of the bulk left to cool down in air after the mixing (Fig. 6) confirmed the hypothesis. Indeed dispersed domains of the CPA minor phase having spherical shape and low adhesion to the PE continuum phase were clearly identified. The dimension of the dispersed phase decreased with lowering the CPA amount in the blend in accordance with the requirement of the system to minimise its free internal energy [33].

The TGA analysis of PE, CPA and of their blends evidenced that the onset temperatures of degradation were higher than 400 °C for all studied materials under the investigated conditions. This result indicated that no degradation process were expected in the experimental conditions adopted during both the mixing in the plastographer and the film compression moulding at 180 or 210 °C.

Table 2
AFM characterisation of the PE pure film compression moulded between aluminium and teflon sheets

| Side | Zoom factor | Height (µm)[a] | Average height (µm)[a] | Peak to peak distance (µm)[a] | Average peak to peak distance (µm)[b] |
|---|---|---|---|---|---|
| Aluminium | 5 | 0.89 | 0.79±0.13 | 1.43 | 1.74±0.47 |
| | 2 | 0.70 | | 1.77 | |
| | 2 | 0.66 | | 1.36 | |
| | 2 | 0.91 | | 2.4 | |
| Teflon | 5 | 2.70 | 2.43±0.49 | 3.1 | 3.23±0.73 |
| | 5 | 2.78 | | 3.65 | |
| | 2 | 2.53 | | 3.91 | |
| | 2 | 1.71 | | 2.25 | |

[a] Average values in a single analysis.
[b] Values averaged out of four successive analysis.

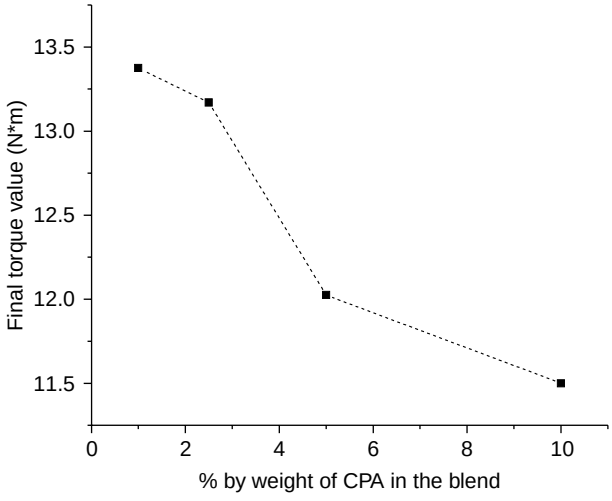


Fig. 4. Final torque value against percentage of CPA in the blend.

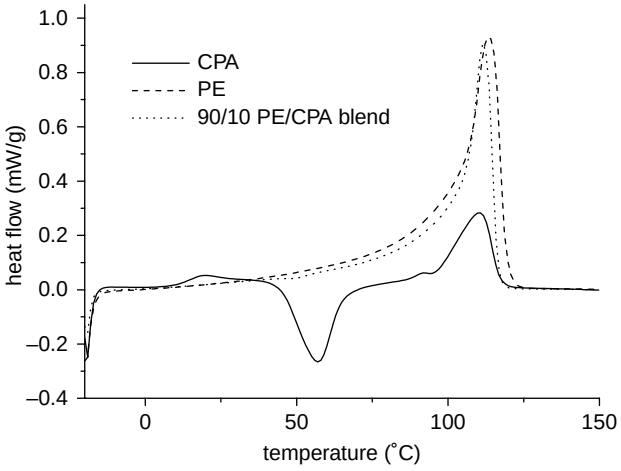


Fig. 5. Comparison between the DSC heating graphic of 90/10 PE/CPA blend and of pure components (PE and CPA).

### 3.4. IR analysis

The surface concentration of CPA as a function of the nature of the material faced during the compression moulding was analyzed by IR spectroscopy. The ratio between the normalized values of the area of the carbonyl absorption peak at 1638 $cm^{-1}$ recorded in reflection and transmission mode were assumed as a measure of the surface concentration of the CPA phase with respect to that in the bulk. The height of the peak at 1377 $cm^{-1}$, which corresponds to the bending mode of the aliphatic chains, was chosen as normalizing value for the spectra recorded both in reflection and transmission in order to delete the ATR and IR spectra dependence on the degree of penetration of the IR ray and on the film thickness, respectively [34,35]. The resulting ratios between the calculated normalized areas of the carbonyl bands in the ATR and FT-IR spectra are then given by Eq. (2), which takes into account the overlapping of CPA and PE bands.

$$\frac{A_{\mathrm{ATR,N}}}{A_{\mathrm{FT-IR,N}}} = \frac{\left(\left(\varepsilon_{\mathrm{CPA}}^{1639} d^{1639} C_{\mathrm{CPA}}^{\mathrm{s}}\right)/\left(\varepsilon_{\mathrm{CPA}}^{1377} d^{1377} C_{\mathrm{CPA}}^{\mathrm{s}} + \varepsilon_{\mathrm{PE}}^{1377} d^{1377} C_{\mathrm{PE}}^{\mathrm{s}}\right)\right)}{\left(\left(\varepsilon_{\mathrm{CPA}}^{1639} l C_{\mathrm{CPA}}^{\mathrm{tot}}\right)/\left(\varepsilon_{\mathrm{CPA}}^{1377} l C_{\mathrm{CPA}}^{\mathrm{tot}} + \varepsilon_{\mathrm{PE}}^{1377} l C_{\mathrm{PE}}^{\mathrm{tot}}\right)\right)} = \frac{d\left(\left(C_{\mathrm{CPA}}^{\mathrm{s}}\right)/\left(\varepsilon_{\mathrm{CPA}}^{1377} C_{\mathrm{CPA}}^{\mathrm{s}} + \varepsilon_{\mathrm{PE}}^{1377} C_{\mathrm{PE}}^{\mathrm{s}}\right)\right)}{\left(\left(C_{\mathrm{CPA}}^{\mathrm{tot}}\right)/\left(\varepsilon_{\mathrm{CPA}}^{1377} C_{\mathrm{CPA}}^{\mathrm{tot}} + \varepsilon_{\mathrm{PE}}^{1377} C_{\mathrm{PE}}^{\mathrm{tot}}\right)\right)} = dR\frac{C_{\mathrm{CPA}}^{\mathrm{s}}}{C_{\mathrm{CPA}}^{\mathrm{tot}}} \tag{2}$$

where $d^{1639}$ and $d^{1377}$ are the penetration depths of the ray at 1639 and 1377 $cm^{-1}$, respectively, and $d$ is the ratio between them. $l$ is the film thickness. $C_{\mathrm{CPA}}$ and $C_{\mathrm{PE}}$ are the concentrations (expressed as fractions) of the blend components at the surface (indicated by the superscript 's') or in the bulk (indicated by the superscript 'tot'). $\varepsilon_{\mathrm{CPA}}^{1639}$ and $\varepsilon_{\mathrm{CPA}}^{1377}$ are the extinction coefficients at the wavelengths reported as superscript and for the substance indicated as subscript. The $R$ parameter, which the equation of is given in (3), depends on the values of the extinction coefficients ($\varepsilon_{\mathrm{CPA}}^{1377}$ and $\varepsilon_{\mathrm{PE}}^{1377}$) and on the PE concentration at the surface and in the bulk.

$$R = \frac{\varepsilon_{\mathrm{CPA}}^{1377} C_{\mathrm{CPA}}^{\mathrm{tot}} + \varepsilon_{\mathrm{PE}}^{1377} C_{\mathrm{PE}}^{\mathrm{tot}}}{\varepsilon_{\mathrm{CPA}}^{1377} C_{\mathrm{CPA}}^{\mathrm{s}} + \varepsilon_{\mathrm{PE}}^{1377} C_{\mathrm{PE}}^{\mathrm{s}}} \tag{3}$$

If $d$ and $R$ are constant values in the condition of analysis, the value of the ratio of Eq. (2) would be proportional to the relative surface concentration of CPA. Indeed, the contribution of CPA to the normalizing band is not zero and then $R$ is not a true constant. By taking into account that the sum of the CPA and PE concentrations must be always equal to 1 both at the surface and in the bulk and by introducing the constant $k$

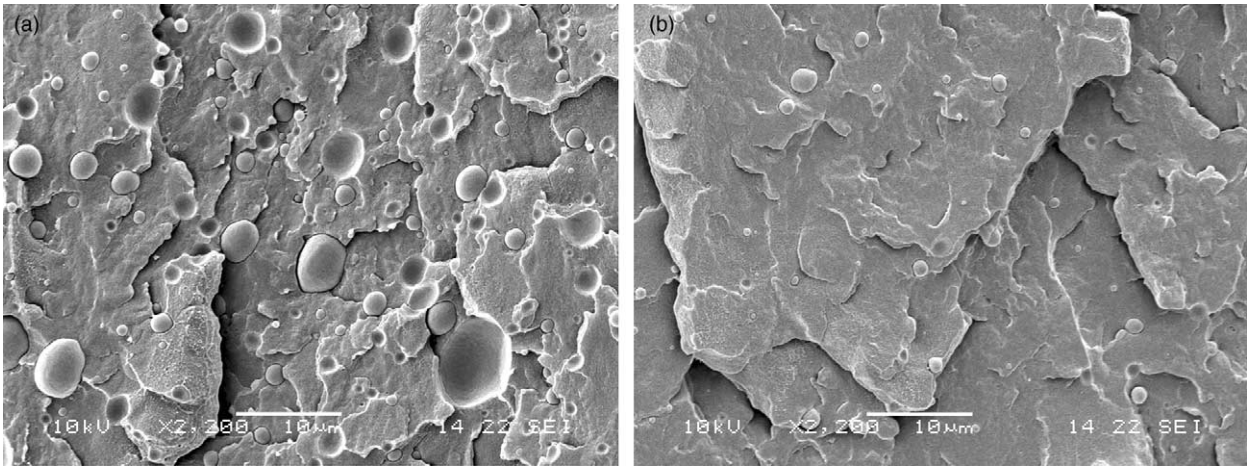


Fig. 6. SEM micrographs of the cryogenic fracture surface of the bulk of PE/CPA blends: 90/10 (a) and 99/1 (b) PE/CPA composition.

defined as $k = \varepsilon_{CPA}^{1377}/(\varepsilon_{CPA}^{1377} - \varepsilon_{PE}^{1377})$, Eq. (3) becomes (4):

$$R = \frac{C_{CPA}^{tot} - k}{C_{CPA}^{s} - k} \quad (4)$$

If the value of 1 for $d$ and the rough value of $-10$ for $k$, which was determined from the IR spectra of pure PE and CPA films, are assumed the relative surface concentration of CPA ($C_{CPA}^{s}/C_{CPA}^{tot}$) can be calculated from Eq. (5) and the normalized ATR and FT-IR experimental absorbance values.

$$\frac{A_{ATR,N}}{A_{FT-IR,N}} = d\frac{1 + (10/C_{CPA}^{tot})}{(C_{CPA}^{s}/C_{CPA}^{tot}) + (10/C_{CPA}^{tot})}\left(\frac{C_{CPA}^{s}}{C_{CPA}^{tot}}\right) \quad (5)$$

The effect of total concentration on the relative surface concentration of CPA in films pressed between two aluminium sheets (Al/Al), or one teflon/one aluminium sheet (Al/T) or two teflon sheets (T/T) was examined (Fig. 7). In the first case the increase of CPA content in the blend is accompanied to a monotonic decrease of the effective CPA surface concentration ($C_{CPA}^{s}/C_{CPA}^{tot}$). The same trend seems to be substantially valid on the aluminium side of the Al/T pressed films apart the 95/5 blend which shows a very high value probably afforded by same experimental errors. The $C_{CPA}^{s}/C_{CPA}^{tot}$ values are higher than for the corresponding blends Al/Al pressed. Accordingly the T face of the Al/T series shows also a substantial monotonic decrease with increasing CPA content and the $C_{CPA}^{s}/C_{CPA}^{tot}$ are smaller than in the two previous cases. In the T/T series the films show a higher similar $C_{CPA}^{s}/C_{CPA}^{tot}$ from 1 to 5% CPA, while drops to the lowest value of all those obtained in the case of the 90/10 PE/CPA blend. Apart from some value irregularities for each blend, the results seem to show that in

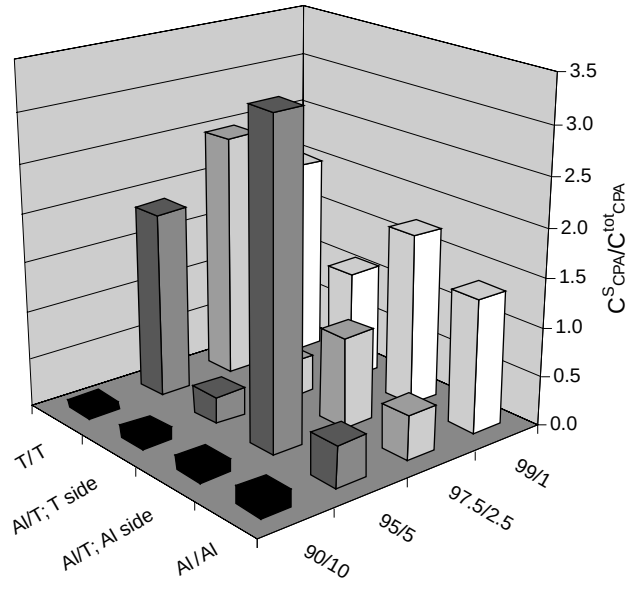


Fig. 7. Relative surface concentration of CPA determined by using Eq. (5) with the values of $-10$ for $k$, 1 for $d$ the normalised absorbance at 1638 $cm^{-1}$ in the ATR and FT-IR spectra of the films compression moulded between aluminium (Al) and/or teflon (T). The PE adsorption at 1377 $cm^{-1}$ was used as normalising band.

Table 3
Water contact angle of films from PE/CPA blends

| Materials[a] | PE/CPA blend composition | | | | |
|---|---|---|---|---|---|
| | 90/10 | 95/5 | 97.5/2.5 | 99/1 | 100/0 |
| | Contact angle [degree] | | | | |
| Aluminium/aluminium | 107 | 95 | 93 | 99 | 98 |
| Aluminium/teflon; aluminium side | 108 | 98 | 95 | 105 | 101 |
| Aluminium/teflon; teflon side | 113 | 98 | 102 | 110 | 107 |
| Teflon/teflon | 116 | 107 | 98 | 107 | 108 |

[a] Nature of the materials faced with the films during their preparation by compression moulding.

average the highest relative surface concentration of CPA is achieved on the aluminium side of the Al/T series.

### 3.5. Contact angle measurement

The contact angle values (Table 3) were higher on teflon than aluminium side surfaces. In any case, all values were higher than 90°, which is the value usually found for hydrophobic flat surfaces like polyolefin films prepared by spin coating [36]. This may be related to the presence of the micro roughness observed by the SEM and AFM analysis on the PE film surfaces (Fig. 3), which are known to increase the surface hydrophobicity (see as example Ref. [37]).

In order to compare the surface hydrophilicity of the films made of blends at different CPA content it was assumed that the patterns of film surfaces faced with equal material during the compression moulding were the same. As a consequence any differences in contact angle values between a blend and a pure PE film faced with equal material can be tentatively assigned to their surface composition.

The relative differences ($\Delta\vartheta = (\vartheta_{PE} - \vartheta_{blend})/\vartheta_{PE}$) of the 99/1 and 95/5 PE/CPA blends indicate a similar wettability (within the experimental error) to PE films (Fig. 8). On the other side the 90/10 and the 97.5/2.5 PE/CPA blends result to be less and more wettable than PE, respectively. No significant difference in wettability was observed for blends having the same PE/CPA ratio moulded between any kind of facing material. The only exceptions are the 97.5/2.5 PE/CPA blend film moulded between two teflon sheets and the teflon side of the 95/5 PE/CPA blend film moulded between teflon and aluminium. This difference is not easy to explain and probably due to possible experimental errors.

### 3.6. SEM investigations

The low CPA concentration near the film surfaces found by IR analysis of the 90/10 blend was confirmed by the SEM observation of the films, which evidenced an average distance of the observable CPA domains larger than the ATR ray penetration (1/1.5 μm) independently of the treatment. The morphology of the films studied by SEM analysis on cryogenic section of PE/CPA 90/10 blend compression moulded for 5 min at 180 °C and 125 bar is shown in Fig. 9 and indicates a strong influence of the polarity of the sheets used for the films

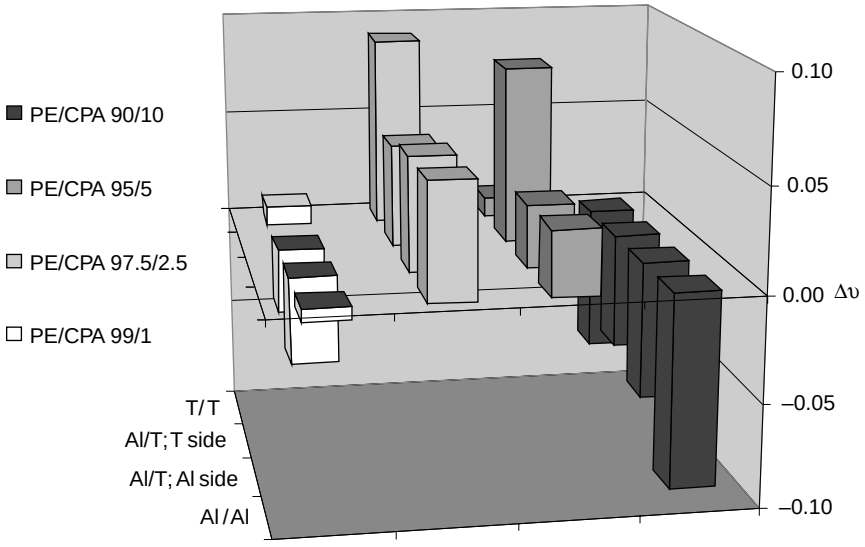


Fig. 8. Relative variation of the contact angle values at the film surfaces of the blends with respect to PE film compression moulded between aluminium (Al) and/or teflon (T): $\Delta\vartheta = (\vartheta_{PE} - \vartheta_{blend})/\vartheta_{PE}$.

preparation. In particular the distribution of the dispersed phase in the film compression moulded between aluminium sheets was homogeneous along the section with a average diameter value of the dispersed phase particles of 6 μm and a maximum value of 20 μm. Non-homogeneous distribution was found if one or two teflon sheets were used for the film preparations. In particular, an enrichment of the CPA phase in the middle of the film section and a gradient distribution with an enrichment of the dispersed phase near the aluminium side was produced in the teflon–teflon and aluminium–teflon compression moulded

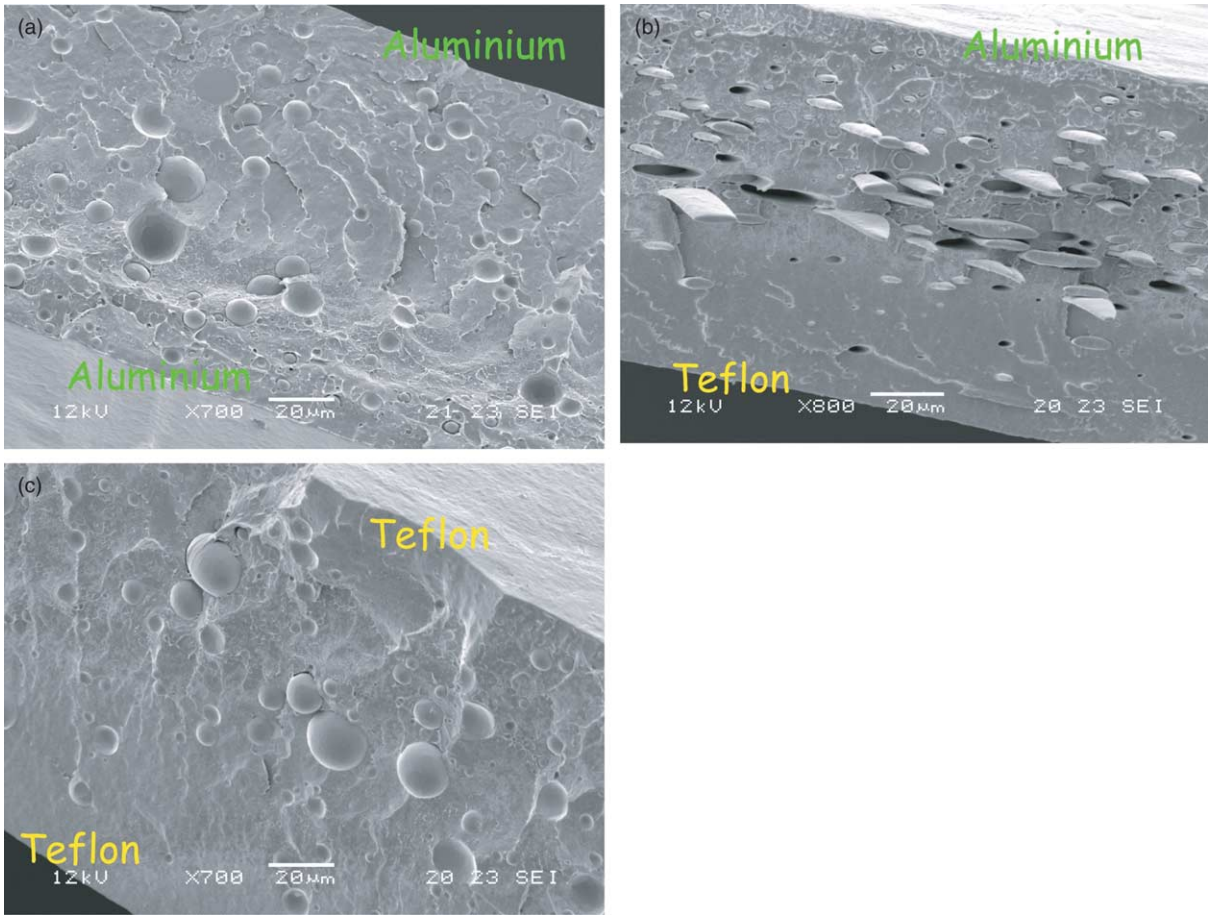


Fig. 9. SEM micrographs of the cryogenic fracture surface of the film made of 90/10 PE/CPA blend compression moulded at 180 °C and 125 bar for 5 min betweem two aluminium sheets (a) between a teflon and a aluminium sheets (b) and between two teflon sheets (c).

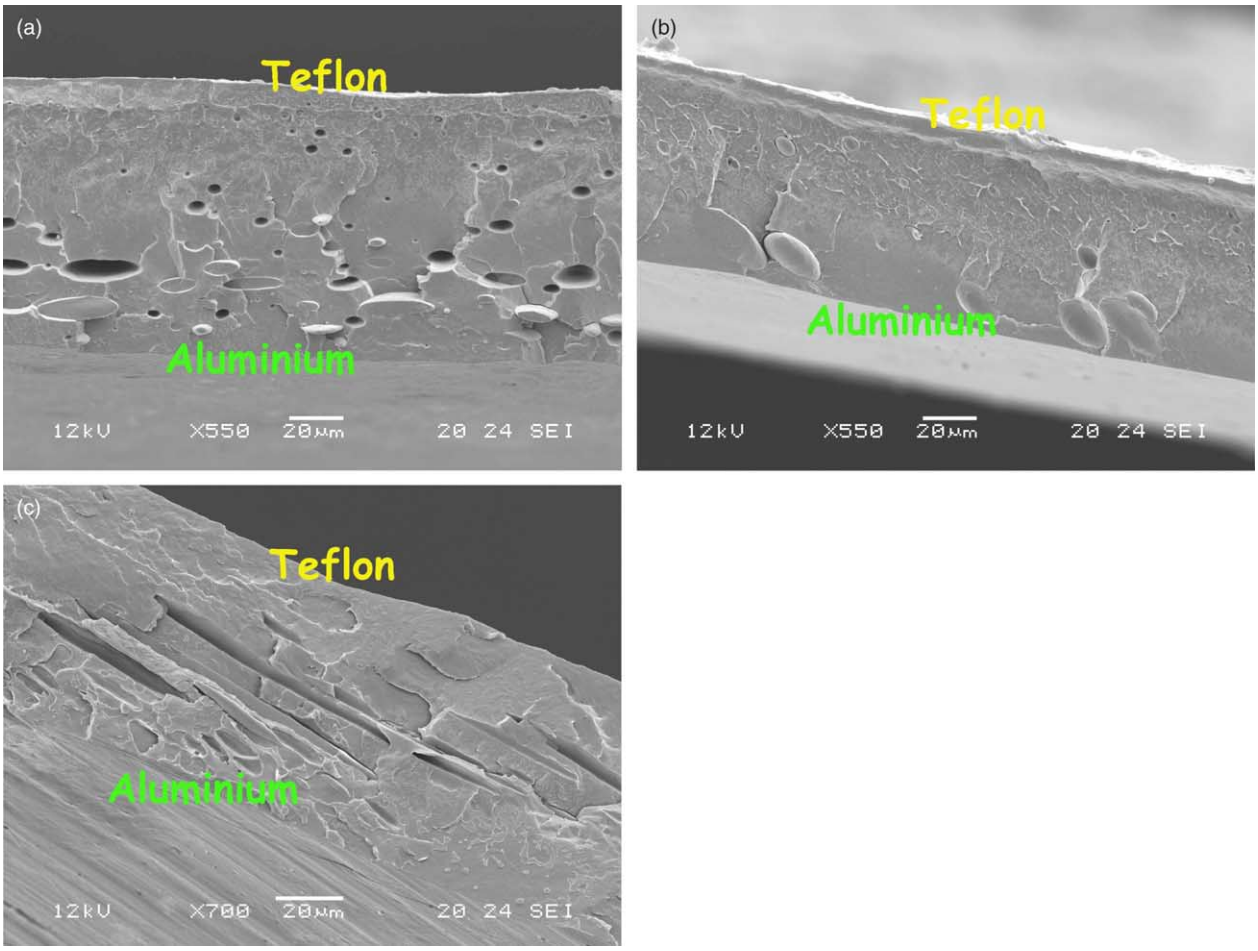


Fig. 10. SEM micrographs of the cryogenic fracture surface of the film made of 90/10 PE/CPA blend compression moulded at 180 °C and 125 bar for 10 min (a) 30 min (b) and 60 min (c).

films, respectively. The dispersed phase exhibited a spherical shape when the films were prepared in symmetric conditions (two teflon or two aluminium sheets) with largest particle diameters (8 μm) when teflon was used instead of aluminium. Otherwise, dispersed phase having an elliptic or lamellar shape was observed (in films compression moulded in asymmetric condition between teflon and aluminium). In addition, the CPA domains were larger in asymmetric conditions than in symmetric ones and their diameter reached even values of 26 μm. The faced material influenced also the minimum distance of the CPA domains from the surface: the value of 10 μm with teflon was reduced to 0.5 μm with aluminium.

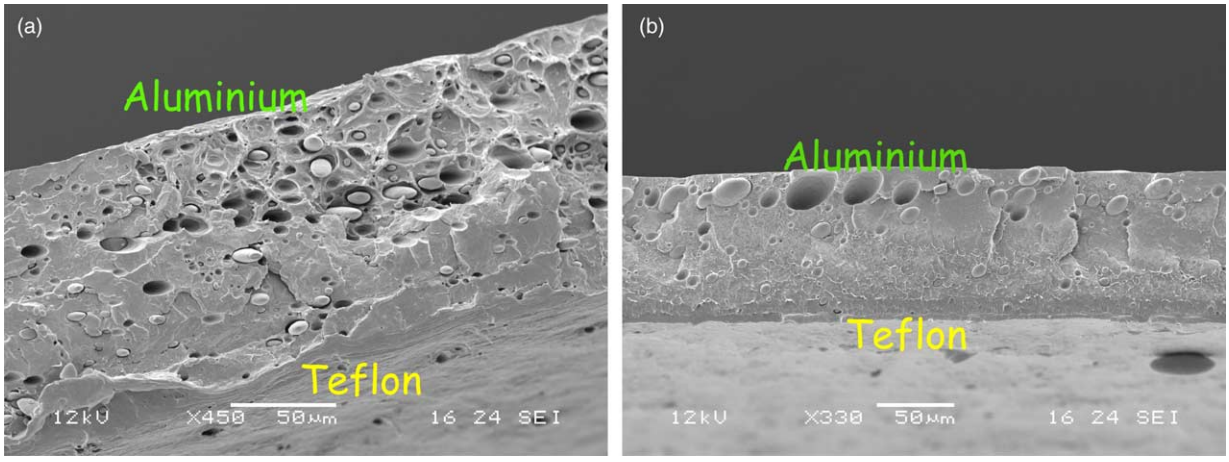


Fig. 11. SEM micrographs of the cryogenic fracture surface of the film made of 90/10 PE/CPA blend compression moulded for 5 min 180 °C and 50 bar (a) or 200 bar (b).

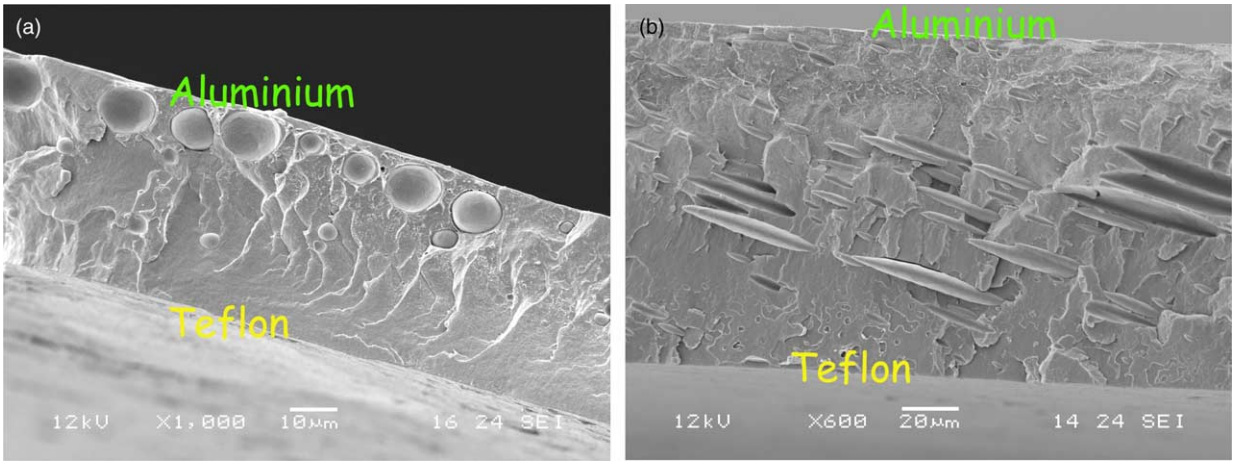


Fig. 12. SEM micrographs of the cryogenic fracture surface of the film made of 90/10 PE/CPA blend compression moulded at 125 bar for 5 min by keeping the temperature of the press plates at: (a) 210 °C the teflon side and 150 °C the aluminium one; (b) 150 °C the aluminium side and 210 °C the teflon one.

The asymmetry in the dispersed phase distribution along the film section did not depend on the position of teflon or aluminium over or below the moulded film.

The energy of adhesion to the aluminium layer of the films compression moulded between teflon and aluminium increased by increasing the moulding time; it was then possible to detach only the edge of the film after 60 min and no detachment was possible after 4 h. The SEM images of the films which could be separated from the aluminium sheet (Fig. 10) showed the tendency of the CPA phase to move towards the aluminium side and at the same time of assuming a lamellar shape while increasing treatment time.

The SEM analysis of the film surfaces did not evidence the presence of large CPA domains and only few cavities were occasionally observed independently of the treatment. Deeper investigation was prevented by the roughness replicated from the surface of either teflon or aluminium sheets. A similar effect was obtained by increasing the pressure during the compression moulding as shown by the SEM picture of the section of the film treated for 5 min at 200 bar between teflon and aluminium (Fig. 11). Poor separation along the section was achieved when 50 bar or no pressure were applied to the films.

A particular non-homogeneous dispersed phase distribution along the section was observed in films compression moulded between teflon and aluminium at 125 bar for 5 min by introducing a temperature gradient. This was actually obtained by keeping one face at 210 °C and the other at 150 °C alternatively (Fig. 12). In particular if aluminium was kept at 150 °C CPA concentrated near the aluminium faced side in elliptic shape domains. On the contrary, if teflon was kept at 150 °C the CPA domains were concentrated mostly on the middle of the film and had a lamellar morphology.

The differences in the phase distribution and morphology observed among the 90/10 PE/CPA films compression moulded between materials with different surface energy were observed also in the films made from the 99/1, 97.5/2.5 and 95/5 PE/CPA blends. These last differed from the first ones only for the number and dimension of the dispersed phase which decreased as the amount of CPA in the blend decreased.

## 4. Discussion

ATR and contact angle data show that the films which show the highest variation of the contact angle do not show the highest CPA concentration at the surface by ATR analysis. In order to explain this apparent contradiction it must be remembered the difference in the depth of penetration of ATR and contact angle measurements which are about 1.5 µm and few angstroms for ATR and contact angle, respectively, at least in the investigation conditions [35,38]. This was confirmed by SEM analysis in the case of 90/10 PE/CPA blend films, where the large amount of the CPA phase allowed a clear identification of the dispersed domains. In this case a linear increasing correlation was found between the average distance of the CPA domains from the film/air interface and the amount of CPA at the surface.

The calculation of the interfacial tension values by the harmonic Wu Eq. (6) on the basis of surface tension data (Table 1) show (Table 4) high value of interfacial tension between PE and CPA, in agreement with the lack of compatibility between the two polymers [40].

$$\sigma_{12} = \gamma_1 + \gamma_2 - \frac{4\gamma_1^{\mathrm{D}}\gamma_2^{\mathrm{D}}}{\gamma_1^{\mathrm{D}} + \gamma_2^{\mathrm{D}}} - \frac{4\gamma_1^{\mathrm{P}}\gamma_2^{\mathrm{P}}}{\gamma_1^{\mathrm{P}} + \gamma_2^{\mathrm{P}}} \tag{6}$$

The substantial preferential segregation of CPA on the film surface faced to aluminium can be also explained considering the interfacial tension values that are higher between teflon and CPA than between aluminium and CPA. The tendency to minimise the energy of the system can be responsible for the asymmetric segregation of CPA. Anyway, the lower values of

Table 4
Interfacial tension values ($\sigma$) calculated by the harmonic Wu Eq. (6)

| Material 1 | Material 2 | $\sigma$ (mN/m) |
|---|---|---|
| PE | CPA | 4.3 |
| Teflon | PE | 8.0 |
| Teflon | CPA | 18.3 |
| Aluminium | PE | 8.5 |
| Aluminium | CPA | 13.9 |

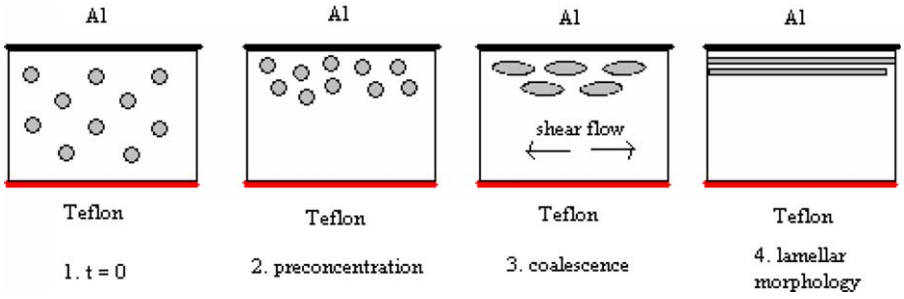


Fig. 13. Simplified scheme of phase morphology development along the film section of films moulded between aluminium (Al) and teflon (T) sheets.

interfacial tension observed between PE and both teflon and aluminium allow to explain the slow CPA surface segregation and the low improvement observed in surface wettability by contact angle measurements. Moreover, the lowest value of interfacial tension was observed for the PE/CPA system, in good agreement with the retaining of the dispersed CPA phase into the bulk during the compression moulding treatment, especially in the blends with higher CPA content.

Long range intermolecular forces can be invoked to explain the observed segregation of CPA in proximity of the aluminium layer. These interactions were reported to be efficient across multilayer systems also over distances up to 125 nm [24]. Films in multilayer structures are destabilized and pattern are formed at interfaces [24]. The same long range forces can be invoked to explain the different blend morphology observed in this study as result of the change in the material of the layer faced above and below the films during its preparation. As result of the presence of these forces the largest destabilizing conditions are attained when asymmetric multilayer geometries are adopted [39].

A complex phase morphology development (see simplified scheme in Fig. 13) along the section of the PE/CPA films was observed by SEM analysis performed on films prepared under different conditions.

By taking into account the polarity and the low molecular weight of CPA, we can assume to start from an immiscible system in which CPA is dispersed as droplets in the PE molten matrix at 180 °C (step 1). The presence of the teflon (T) and aluminium (Al) sheets induces the preferential migration of droplets towards the aluminium sheet on the basis of interfacial tension values. This creates a pre-concentration of CPA in the aluminium side of the film. In this region, the local composition of CPA in the blend is higher and coalescence phenomena are favoured also by the decrease of the local blend viscosity [41] giving elongated domains. The presence of a shear rate, due to the higher compression of the material in proximity of the solid layers [6], favours the formation of elongated structure (Figs. 10 and 11). The lamellar and/or fibre-like interconnected obtained after 1 h of moulding can be the consequence of the attaining of the percolation threshold as the consequence of CPA enrichment in the proximity of the Al layer [42].

An increase of mechanical pressure can favour the pre-concentration, because of the higher shear stress, which allows a faster morphology assessment. On the other side the presence of a higher temperature on the teflon side favours the pre-concentration step because it creates a gradient of viscosity along the section. The migration of CPA domains in the teflon side towards the Al side in a medium with lower viscosity is thus favored. On the contrary a lower temperature on the teflon side gives an opposite gradient. In this way the migration of the CPA domains from the teflon side to the Al side is prevented. Hence elongated structure are observed exclusively in the asymmetric moulding system because only in this case a pre-concentration step is possible due to long range intermolecular forces. Moreover, the elongated structures formation can be also favoured by the particular low viscosity and low elasticity in the melt of CPA [43] and by the quenching step performed at −20 °C, which can allow a competition among PE crystallization and CPA domains break-up [44].

## 5. Conclusion

The energy and the interactions at the surfaces of a moderately thick film from a blend of linear low density polyethylene and low molecular weight copolyamide produced non-homogeneous phase distribution in the direction perpendicular to the film main surface. In particular the polar component CPA (the dispersed phase) enriches near the film side contacted with a polar surface provided by an aluminium sheet. An opposite effect is provided by teflon which has low surface energy and then does not strongly interact with the polar component of the blend.

The shape, the dimension and the distribution of the CPA dispersed domains depended on treatment conditions such as temperature, pressure, time and kind of surfaces used during the compression in a parallel plate heating press. In particular a spherical shape is allowed when two equal surfaces were used (teflon or aluminium) whereas a lamellar shape were produced with asymmetric surface interactions using teflon and aluminium sheets. The dispersed phase was mostly concentrated in the middle of the film obtained between two teflon sheets, whereas was homogeneously distributed along the section of the film compression moulded between two aluminium sheets. A gradient distribution along the section was observed when two different surfaces (aluminium and teflon) were used with a higher copolyamide concentration near the aluminium side. The eliptical copolyamide domains produced by asymmetric interactions resulted to evolve with the treatment time to a layered morphology with the most polar

blend component concentrated at the aluminium surface as indicated by the increasing peeling strength.

The phase morphology development along the section can be tentatively explained by a combination of different effects such as long range intermolecular forces and shear stress caused by the compression process. In conclusion the results indicated here can be useful to design a possible strategy to prepare self adhesive polyolefin based material by simply mixing a low viscosity polar polymer to polyethylene during its processing.

## Acknowledgements

The authors would like to thank Prof Francesco Ciardelli for useful discussion and revising the manuscript. Gruppo x di x Gruppo (Venezia, Italy) for providing chemicals. Partial support by Alcan Packaging (Lugo di Vicenza, Italy) and MIUR (Ministero dell'Istruzione, Università e Ricerca) is here acknowledged.

## References

[1] Garbassi F, Morra M, Occhiello E. Polymer surfaces, from physics to technology. Chichester, England: Wiley; 1996.
[2] Gonzalez-Montiel A, Keskkula H, Paul DR. Polymer 1995;36:4587.
[3] Kudva RA, Keskkula H, Paul DR. Polymer 1999;40:6003.
[4] Thomas S, Groeninckx G. J Appl Polym Sci 1999;71:1405.
[5] Fellahi S, Favis BD, Fisa B. Polymer 1996;37:2625.
[6] Verfaillie J, Devaux J, Legras R. Polymer 1999;40:2929.
[7] Moffit M, Rharbi Y, Li H, Winnik M. Macromolecules 2002;35:3321.
[8] Moffit M, Rharbi Y, Li H, Winnik M, Tong J, Farina J. J Polym Sci, Polym Phys 2003;41:637.
[9] Opdahl A, Phillips RA, Somorjal GA. J Polym Sci, Polym Phys 2003;42: 421.
[10] Takeno H, Nakamura E, Hashimoto T. J Chem Phys 1998;110(7):3612.
[11] Lipatov YS. Prog Polym Sci 2002;27:1721.
[12] Geoghegana M, Krauschb G. Prog Polym Sci 2003;28:261.
[13] Cherrabi R, Saout-Elhak A, Benhamou M, Daoud M. J Phys Chem 1999; 111(17):8174.
[14] Heier J, Kramer E, Revesz P, Battistig G, Bates FS. Macromolecules 1999;32:3758.
[15] Sheffold F, Eiser E, Budkowski A, Steiner U, Klein J, Fetters LJ. J Chem Phys 1996;104(21):8786.
[16] Cao D, Wu J. Macromolecules 2005;38:971.
[17] Huggins AM, Jones RAL. Nature 2000;404:476.
[18] Kokkinos IG, Kosmas MK. Macromolecules 2003;36:6252.
[19] Coulon G, Daillant J, Collin B, Bennattar JJ, Gallot Y. Macromolecules 1993;26:1582.
[20] Indrakanti A, Jones RL, Kumar SK. Macromolecules 2004;37:9.
[21] Boltau M, Walheim S, Mlynek J, Krausch G, Steiner U. Nature 1998;391: 877.
[22] Opdahl A, Phillips AR, Somorjai AG. J Poly Sci, Polym Phys 2004;42: 421.
[23] Morarium DM, Schäffer E, Steiner U. Phys Rev Lett 2004;92(15):1.
[24] Reiter G, Sharma A, Casoli A, David MO, Khanna R, Auroy P. Languimir 1999;15:2551.
[25] David MO, Reiter G, Sitthaï T, Schultz J. Languimir 1998;14:5667.
[26] Bucknall DG. Prog Mater Sci 2004;49:713.
[27] Takahara A, Kawaguchi D, Tanaka K, Tozu M, Hoschi T, Kajiyama T. Appl Surf Sci 2003;204:538.
[28] Chen J, Zhuang H, Zhao J, Gardella Jr JA. Surf Interface Anal 2001;31: 713.
[29] Schmidt JJ, Gardella Jr JA, Salvati Jr L. Macromolecules 1989;22:4489.
[30] Clark Jr MB, Burkhardt CA, Gardella Jr JA. Macromolecules 1989;22: 4495.
[31] Brant P, Karim A, Douglas JF, Bates FS. Macromolecules 1996;29:5628.
[32] Cassie A. Discuss Faraday Soc 1948;74:5041.
[33] Utraki LA. Polymer alloy and blends. Munich: Hanser Publishers; 1989.
[34] Harrick NJ. Internal reflection spectroscopy. New York: Wiley; 1979 p. 30.
[35] Mirabella FM, editor. Internal reflection spectroscopy: theory and applications. Practical spectroscopy; 1993.
[36] Adamson AW, Gast AP. Physical chemistry of surfaces. 6th ed. New York: Wiley; 1997 [chapter 10].
[37] Yoshimitsu Z, Nakajima A, Watanabe T, Hashimoto K. Langmuir 2002; 18:5818.
[38] Stamm M. Advance in polymer science. vol. 100. Berlin: Springer; 1992.
[39] Ivanov IB. Thin liquid films: fundamentals and applications. New York: Marcel Dekker; 1988.
[40] Guerrica-Echevarria G, Eguiazabal JI, Nazabal J. Polym Test 2000;19: 649.
[41] Serpe G, Jarrin J, Dawans F. Polym Eng Sci 1990;30(9):553.
[42] Potschke P, Paul DR. J Macromol Sci, Polym Rev 2003;C43(1):87.
[43] Harrats C, Groeninckx G. In: Ciardelli F, Penczek S, editors. Modification and blending of synthetic and natural macromolecules. Dordrecht: Kluwer Academic Publishers; 2004. p. 155.
[44] Deyrail Y, Fulchiron R, Cassagneau P. Polymer 2002;43:3311.